



# Viscoplastic Deformation, Stress and Strain Paths in Unconsolidated Reservoir Sands (Part 2): Field Applications Using Dynamic DARS Analysis

Chan, A.W.

*Department of Geophysics, Stanford University, Stanford, CA, USA*

Hagin, P.N. and Zoback, M.D.

*Department of Geophysics, Stanford University, Stanford, CA, USA*

Copyright 2004, ARMA, American Rock Mechanics Association

This paper was prepared for presentation at Gulf Rocks 2004, the 6<sup>th</sup> North America Rock Mechanics Symposium (NARMS): Rock Mechanics Across Borders and Disciplines, held in Houston, Texas, June 5 – 9, 2004.

This paper was selected for presentation by a NARMS Program Committee following review of information contained in an abstract submitted earlier by the author(s). Contents of the paper, as presented, have not been reviewed by ARMA/NARMS and are subject to correction by the author(s). The material, as presented, does not necessarily reflect any position of NARMS, ARMA, CARMA, SMMR, their officers, or members. Electronic reproduction, distribution, or storage of any part of this paper for commercial purposes without the written consent of ARMA is prohibited. Permission to reproduce in print is restricted to an abstract of not more than 300 words; illustrations may not be copied. The abstract must contain conspicuous acknowledgement of where and by whom the paper was presented.

**ABSTRACT:** Utilizing a modified Cam clay cap model, we have transformed laboratory measurements of the stress-dependency of unconsolidated deformation to reservoir space (i.e., in terms of in-situ stress and pore pressure) such that changes in both stress and strain can be assessed as a function of depletion. In previous studies, this transformation, which we term Deformation Analysis in Reservoir Space (DARS), has been performed based on static laboratory experiments. Although this static approach yields a reasonable first order approximation of total deformation, it fails to capture the effects of the change in production rate and the time-dependency of inelastic deformation associated with depletion in unconsolidated reservoirs. To address time-dependent deformation (e.g., creep strain), we have incorporated Perzyna viscoplasticity theory to the modified Cam clay cap model. Following the procedure described by Hagin and Zoback in the accompanying paper, the threshold compaction pressure as a function of strain rate is determined from basic hydrostatic compression tests. As strain rate can also be expressed as a function of production rate, the static DARS can now be extended into a dynamic formalism that predicts the change in physical properties such as porosity reduction, permeability reduction and changes in rock properties associated with production.

## 1. INTRODUCTION

In a depleting reservoir, the reduction in pore pressure can induce marked reductions in porosity leading to compaction (and possibly subsidence), and potentially significant reductions in permeability. Thus, understanding the relationship between production, compaction and permeability loss is an important factor in reservoir management. For most weak sand reservoirs, both elastic and inelastic deformations occur during production. While most reservoir deformation models are based on poroelasticity theory, the impact of viscoplasticity on reservoir deformation cannot be ignored [e.g., 1,2]. In this paper, we will first review standard formalism we termed as Deformation Analysis in Reservoir Space (DARS) in previous

studies [3]. Incorporating the viscoplastic theory, we will then extend the standard DARS from a static analysis to a dynamic analysis that characterizes both instantaneous and time-delayed deformations in terms of reservoir compaction and the associated permeability changes. We will also present a plausible relationship between porosity reduction and permeability change during reservoir depletion based on laboratory experiments. This relationship will then be applied to our case studies to demonstrate how permeability can be estimated in a producing reservoir.

A number of laboratory studies of the dependency of permeability on porosity, stress and deformation mechanism have been published. Zhu and Wong [4] suggested that permeability and porosity changes for most low-porosity sandstones closely track one

another in the cataclastic flow regime. However, a drastic change in permeability was triggered by the onset of shear-enhanced compaction once the sample is loaded beyond the elastic domain into the plastic deformation domain in the reservoir stress space. The effects of plastic deformation and permeability alteration can be extremely significant in reservoir simulations of a highly compressible reservoir [5]. Using coupled simulations, Yale [5] shows that the initial stress state and plasticity significantly increased the compressibility of the formation and the compaction drive energy of the reservoir; while modeling the changes in permeability with plastic deformation shows an extremely large effect on near wellbore pressure drawdown and deformation over normal simulations. Crawford and Yale [6] used an elastoplastic model (also refer to as critical state model) to study the relationship between deformation and the corresponding permeability loss. They showed that an elastoplastic model could capture the main characteristics of the experimental results in which permeability changes with both stress and strain follow a similar constitutive model as deformation for a weak sandstone sample and an unconsolidated sand samples.

Although laboratory experiments on the stress dependency of porosity and permeability are conducted frequently, the stresses used in the laboratory tests (mean stresses and shear stresses) cannot be measured directly in the reservoir. A bridge between the laboratory and in-situ environments is required. Utilizing laboratory experiments along with in-situ stress measurements, Deformation Analysis in Reservoir Space (DARS) can be used for monitoring the evolution of a deforming reservoir in terms of compaction, and production-induced normal faulting [3].

## 2. DEFORMATION ANALYSIS IN RESERVOIR SPACE (DARS)

The principal idea of DARS is to bridge simple laboratory compaction measurements with *in-situ* stress measurements to predict reservoir deformation associated with depletion. This formalism provides a straightforward method to assess how a reservoir will deform with depletion and considers both compaction and induced faulting. While the existing DARS formalism for reservoir deformation failed to capture the time-dependent component of reservoir deformation

associated with weak sand (e.g., creep), we introduce a dynamic version of DARS to incorporate the Power Law Creep Model derived by Hagin [7] to extend the applicability of DARS to weakly consolidated reservoirs. With the inclusion of the creep component, we can then predict the amount of compaction within a weak sand reservoir more accurately.

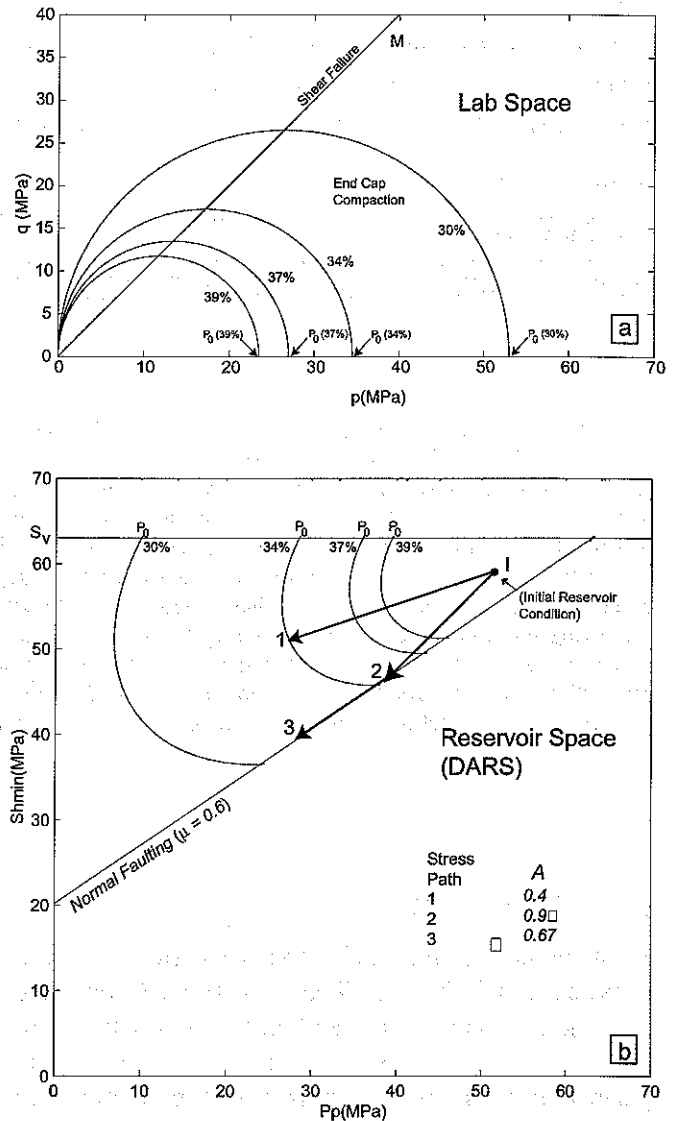


Figure 1: The transformation of end caps from laboratory space ( $p$ - $q$ ) into reservoir space ( $S_{hmin}$ - $P_p$ ) based on the Cam-Clay model (after Chan & Zoback, 2002). (a) Schematic diagram in laboratory space showing the changes in porosity of a rock sample as a result of changes in pressure where  $p$  is the mean stress and  $q$  is the deviatoric stress. (b) The transformed end caps in reservoir space. Stress paths 1, 2 and 3 are possible stress paths that a depleting reservoir may follow.

There are four essential steps to construct the Standard DARS formalism (See [3] for more detailed discussion):

- (i) Laboratory measurements of porosity and permeability reduction as a function of pressures are needed.
- (ii) If only hydrostatic experiments are available, theoretical plasticity model can be utilized to extrapolate these data into  $p:q$  space and then into reservoir space. A Cam-Clay model was used in our studies because of its simplicity.
- (iii) The initial stress state in the reservoir must be measured.
- (iv) The reservoir stress path must be estimated, either using poroelastic theory or empirical observations.

Mathematically, the Cam-Clay model stated that

$$M^2 p^2 - M^2 p_0 p + q^2 = 0 \quad (1)$$

where  $p$  is the mean stress,  $q$  is the deviatoric stress,  $p_0$  is the threshold pressure and  $M$  is the critical state line. For the Standard DARS, this threshold pressure refers to the confining pressure corresponding to a given porosity (or volumetric strain) under a uniaxial experimental setting. A spontaneous change in porosity can then be estimated from this static approach (Figure 1).

For stress changes larger than the yield stress (or preconsolidation pressure in the reservoir), the overstress will then be translated into the Perzyna viscoplastic relationship [7, 8]. The Perzyna viscoplasticity model suggests that the total strain-rate can be divided into elastic and viscoplastic component. Hagin & Zoback [8] derived the empirical viscoplastic relationship for unconsolidated sand from the Wilmington field such that:

$$\dot{\epsilon}_{vp} = 2.36 \times 10^{-13} p_{os}^{6.58} \quad (2)$$

where  $p_{os}$  is the overstress. The change in porosity as a result of viscoplastic effect can then be estimated once the overstressed and lag-time are determined.

Total strain derived by combining both the spontaneous and time-delayed volumetric strain can then be determined and could yield a more accurate estimation on porosity change as a result of production in a weak sand formation.

### 3. LABORATORY EXPERIMENTS ON COMPACTION AND PERMEABILITY LOSS

As reservoir depletion occurs, decreases in pore pressure as a result of production will increase the effective stresses within the reservoir. The increasing effective stresses acting on the formation materials will lead to progressive states of deformation when the material's failure limits are reached. Deformation such as compaction and grain rearrangement (and eventually grain crushing and pore collapse) are the dominant deformation mode for poorly consolidated or unconsolidated sediments when the mean effective stresses are significantly higher than the deviatoric effective stresses. These ductile yielding behaviors of rocks are represented by end caps (or yield caps) in the laboratory domain (mean stress vs. deviatoric stress, or  $p:q$  space). The shape of these end caps corresponds to the same volumetric plastic strain acting on the sample and the criterion model chosen [9].

Laboratory experiments on samples collected from a Gulf of Mexico reservoir in the previous study were used for determining the stress dependency of porosity and permeability [3]. When examining laboratory experiments, marked changes in the rate of reduction may occur (e.g. samples from the GOM Field X used in Chan & Zoback [3]). Chan & Zoback [3] termed the marked change in porosity and permeability as the 'deformation threshold'. The pressure at which such drastic change in the samples occurs coincides with the theoretical preconsolidation pressure. This theoretical preconsolidation pressure is the largest pressure the formation is expected to experience during burial. In the Gulf of Mexico, such pressure can be estimated as the effective vertical stress under hydrostatic pressure. When the sample is loaded beyond this preconsolidation pressure, it is expected to deform as if it is under natural burial compaction.

As porosity reduced during depletion, permeability of the compacting formation also decreased. Chan and Zoback [3] compared the experimental results on porosity changes and the associated permeability changes for 22 deep-water turbidites samples from across the Gulf of Mexico basin reported by Ostermeier [10]. The two bounds seem to provide reasonable estimations of compaction-induced permeability loss for most reservoirs in the Gulf of Mexico (Figure 2).

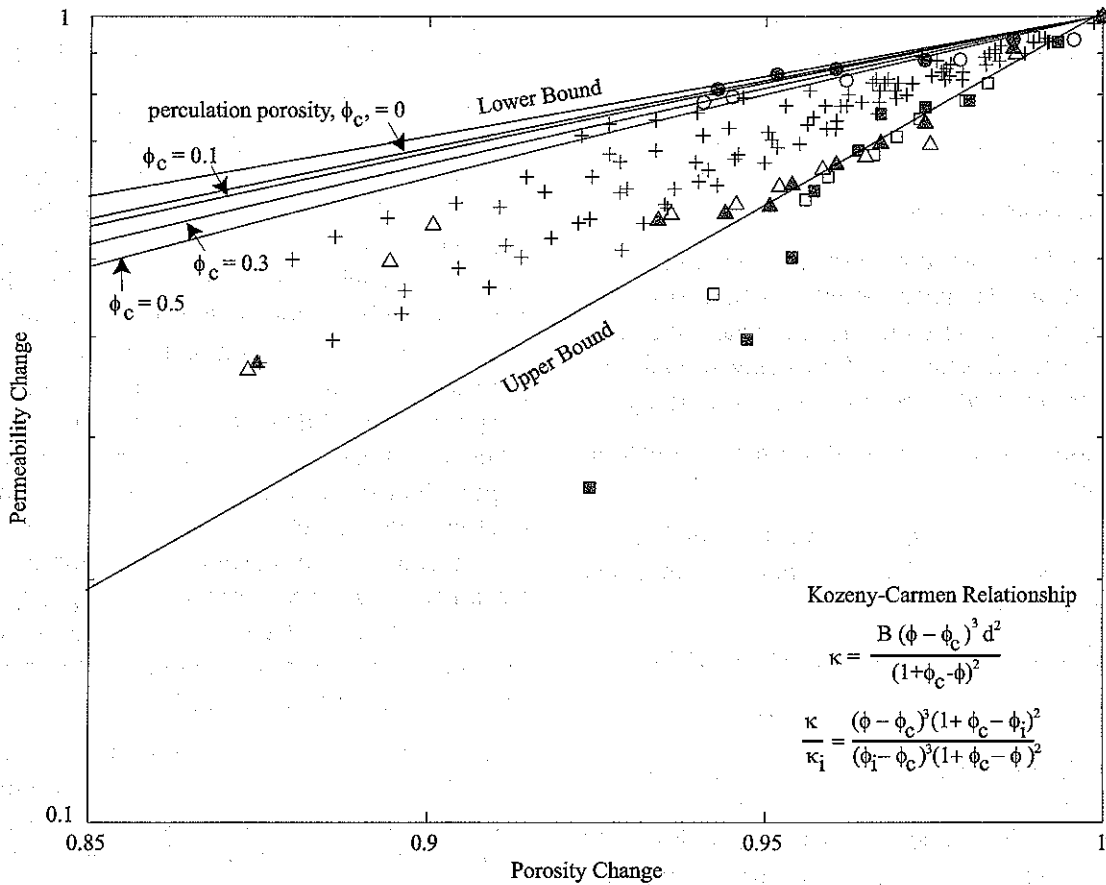


Figure 2: Comparing the empirical permeability-positivity relationship derived from several laboratory studies (modified after [3]) with the well-documented Kozeny-Carman relationship. The data points and the two trends are interpretations used in Chan & Zoback's first attempt to study the effect of compaction on permeability. The red lines are derived based on the modified Kozeny-Carman relationship. Note the similarity between the empirical lower bound and the Kozeny-Carman relationship with no percolation porosity. As a result, it is plausible to use Kozeny-Carman relationship to estimate permeability change as a result of compaction for highly permeable sands. However, Kozeny-Carman relationship cannot characterize the majority of the data and can therefore used as a reference for the lower bound of permeability change.

The Kozeny-Carman relationship is a widely used method to determine permeability of a porous formation in terms of generalized parameters such as porosity [11,12]. Derived from Darcy's Law and laminar flow through circular pipe, the Kozeny-Carman states that

$$k = \frac{B\phi^3}{\tau^2 S^2} = B\phi^3 \frac{d^2}{\tau} \quad (3)$$

where  $k$  is permeability,  $B$  is a geometric factor,  $\tau$  is tortuosity and  $d$  is the typical grain diameter. The porosity,  $\phi$ , and the specific surface area,  $S$ , can be expressed by:

$$\phi = \frac{\pi R^2}{A} \quad \text{and} \quad S = \frac{2\pi R}{A} \quad (4)$$

Mavko and Nur [13] suggested that percolation porosity,  $\phi_c$ , might control the threshold porosity that determines the permeability of the material. The percolation porosity is defined as the limiting porosity at which the existing pores within the formation are disconnected and do not contribute to flow. The modified Kozeny-Carman relationship that includes the percolation porosity becomes:

$$k = B \frac{(\phi - \phi_c)^3}{(1 + \phi_c - \phi)^2} d^2 \quad (5)$$

where  $\phi_c$  ranged from 0 to 0.05 in most cases.

To determine the permeability loss as a result of porosity changes using the modified Kozeny-

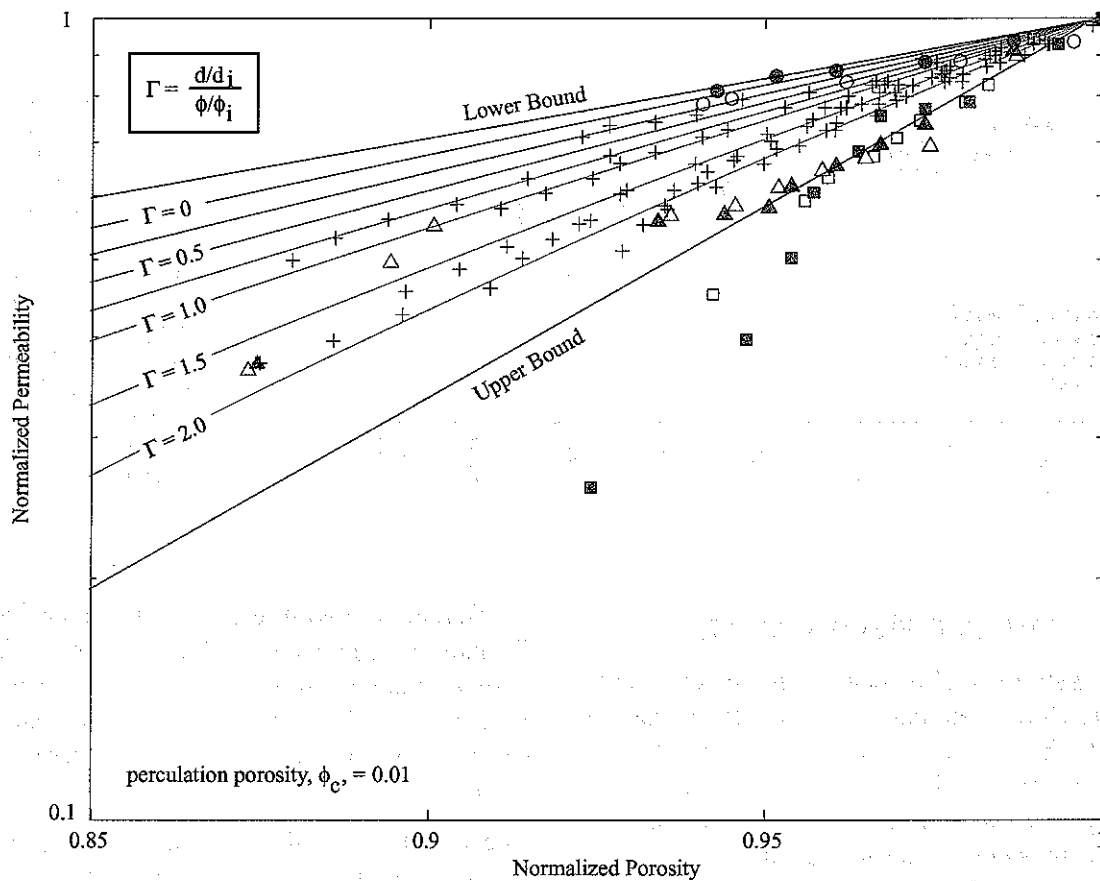


Figure 3: Assuming grain-size reduction occurring during compaction, the modified Kozeny-Carman relationship can describe more data that fall near the upper bound. However,  $\Gamma = 1$  or higher is highly unlikely. Grain-size reduction alone cannot be used to explain the drastic changes in permeability reduction in some samples (or the Upper Bound of permeability loss).

Carman relationship simplifies Equation 5 such that both geometric factors are removed:

$$\frac{k}{k_i} = \left( \frac{\phi - \phi_c}{\phi_i - \phi_c} \right)^3 \left( \frac{1 + \phi_c - \phi_i}{1 + \phi_c - \phi} \right)^2 \quad (6)$$

where  $k_i$  and  $\phi_i$  are the initial permeability and initial porosity respectively. The theoretical values of compaction-induced permeability changes for  $\phi_c$  ranging from 0 to 0.05 using Equation 6 are then superimposed onto the laboratory data from the GOM core samples (Figure 2). The theoretical permeability changes from the modified Kozeny-Carman relationship are similar to the lower bound estimated from the laboratory data. This similarity might imply that the empirical lower bound represents the lower limit of permeability changes for most GOM sands for which percolation porosity does not exist. In other words, if the producing formation is composed of porous materials in which

all pore spaces are well connected, the Kozeny-Carman relationship with  $\phi_c = 0$  could be used as a reference for the lower limit of permeability changes as a result of production-induced compaction. The permeability change estimation from the Kozeny-Carman relationship stated in Equation 6 assumes a constant grain size during compaction and cannot fully capture the significantly large permeability loss due to compaction. The modified Kozeny-Carman relationship alone cannot be used to describe the effect of permeability loss due to compaction in weak sediments. We explored the potential impact of grain-size reduction on permeability estimation based on the modified Kozeny-Carman relationship. Although grain-size reduction does have some influence on the permeability reduction, Figure 3 shows that a very high grain-size reduction is required to explain the upper bound of permeability loss.

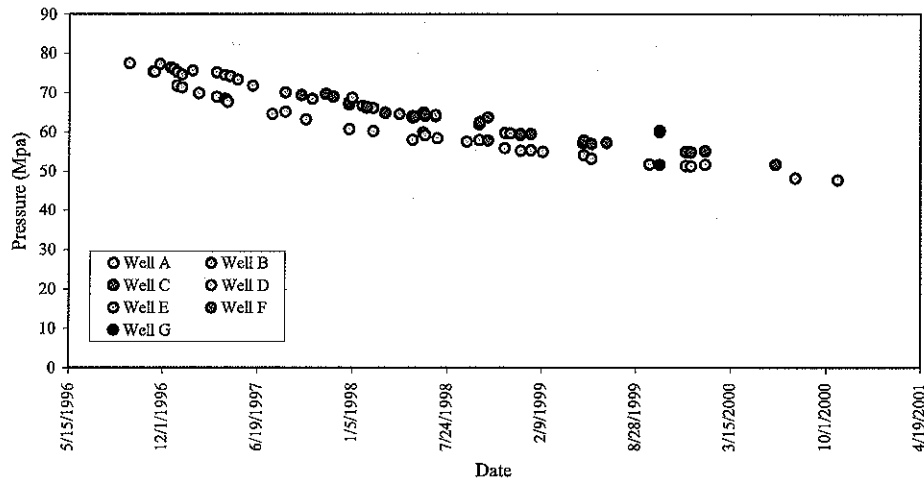


Figure 4: Pressure data for Field Z. Two trends are observed suggesting well A penetrated a different sub-compartment than the rest of the wells. Since the reservoir generally depletes as a single unit, stress measurements from most wells can be used to determine the depletion stress path. In addition to the stress measurements, in-situ permeability measurements are available for wells A, B and C.

#### 4. GULF OF MEXICO FIELD X AND Z

Gulf of Mexico Field X is located on the continental shelf of the Gulf Coast basin off the Texas coast. It is one of the several fields along the Lower Miocene normal growth fault trend. The reservoir is trapped by a fault and its associated rolled-over anticline with sand expansion as a result of the growth fault and thinning from the crest to the anticline. The sand is deltaic and has a porosity ranging from 18 to 33%. The initial permeability ranged from 10 to 300md. The discovery well was drilled in 1980 and the field went into production in 1985 with an initial gas column of over 220 m and initial pressure of about 82 MPa.

GOM Field Z is a deepwater Pliocene to Miocene over-pressured reservoir juxtaposed against a large salt dome. Discovered in the late 1980s, Field Z has been in production since the mid 1990s. The formation is mainly turbidite sands with an average porosity of 30%. The succession of several fining upward sequences resulted in a variation of reservoir quality. Initial horizontal permeability of the sands ranged from 60 to 168 mD for a moderate quality sand and 350 to 540 mD for a good quality sand interval. Both laboratory and  $S_{hmin}$  measurements are available in this field. In addition to the stress measurements, horizontal permeability measurement is also available in Field Z.

Pore pressure measurements from most wells in the region were compiled and corrected to a datum and a continuous decrease in  $P_p$  and the least principal stress can be observed (Figure 4). From the pressure data, reservoir pressure from Well A declines along

a different path with respect to the other wells in the formation suggesting the existence of sub-compartmentalization within the formation. The nature of the sub-compartmentalization that separated Well A to the rest of the reservoir is not clear.

The evolution of the  $S_{hmin}$  and  $P_p$  is presented in Figure 5. Similar to Field X reported in Chan and Zoback [3], the relatively low stress path in Field Z,  $A = 0.54$ , suggests that production-induced normal faulting is unlikely to occur. In other words, the initial stress state was one in which normal faults were active, depletion caused these faults to stabilize.

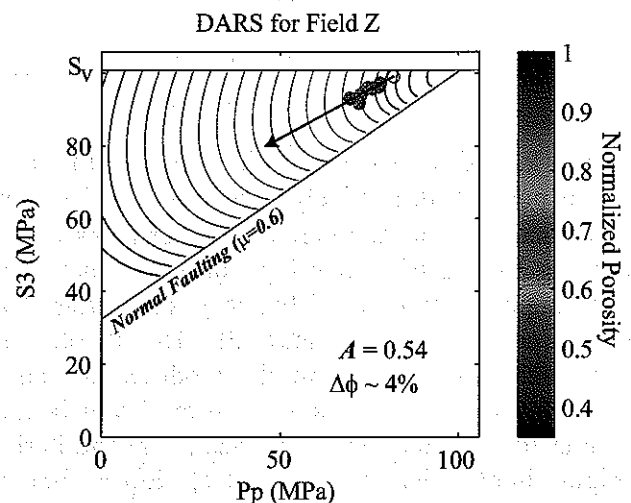


Figure 5: DARS for Field Z. The relatively low stress path of 0.54 in Field Z suggests that production-induced normal faulting is unlikely to occur. Using available laboratory experiments, DARS predicted a 4% change in porosity.

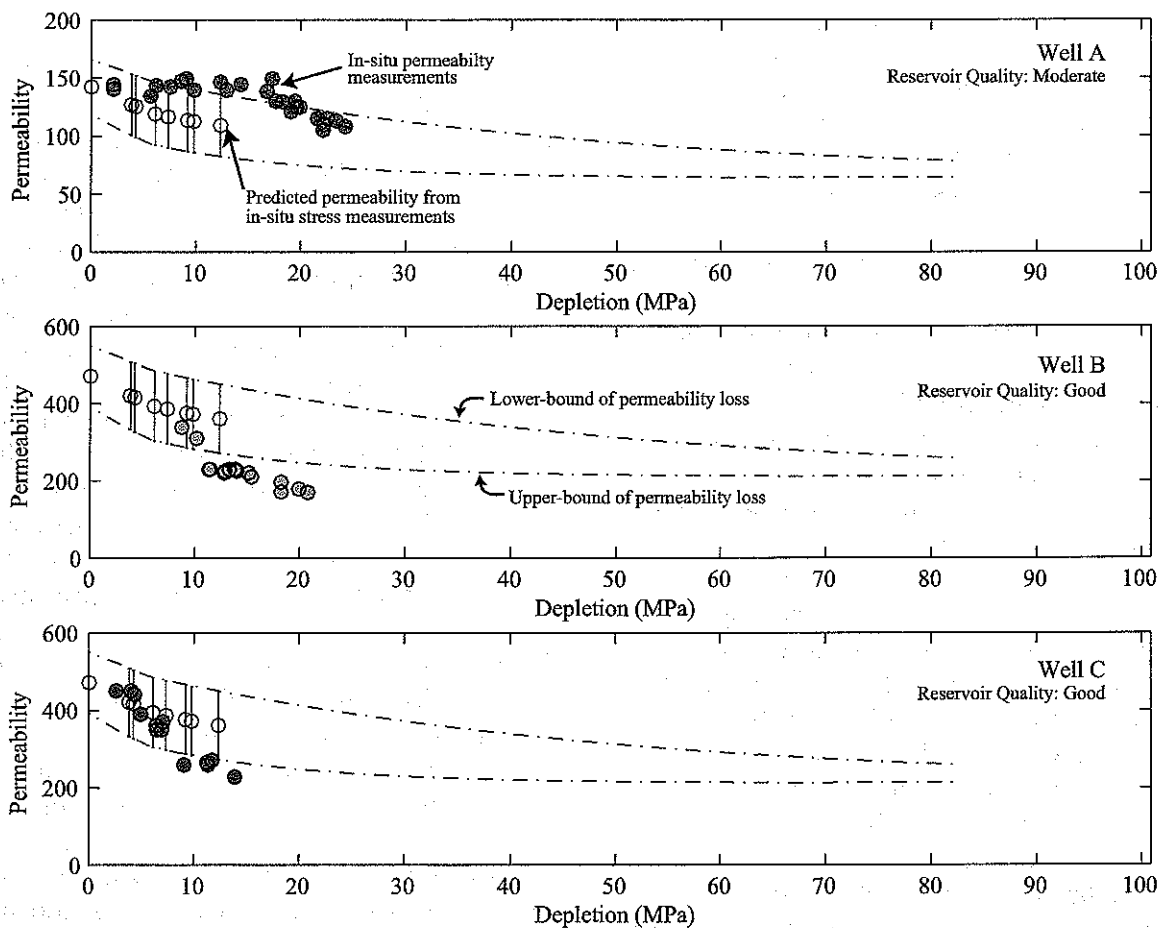


Figure 6: Comparison between in-situ permeability measurements from wells A, B and C with the predicted permeability using DARS and the empirical porosity-permeability relationship. The blue open circles are the predicted average permeability values corresponding to the in-situ stress measurements. The two blue lines are the lower and upper bounds of permeability loss assuming the reservoir will deplete along the same stress path. The color-filled circles are in-situ stress measurements from the 3 wells. Initial permeability measurements from these wells are not available; estimations based on reservoir properties are used as reference points.

Laboratory experiments on rock compressibility are available for GOM Field Z and are used in the DARS study. Unlike the sample from Field X, a marked decrease in porosity similar to that reported by Chan & Zoback [3] is not observed from this Field Z sample. The absence of a drastic change in this sample may be related to the much greater depth, or greater preconsolidation pressure, experienced by the sample. However, more laboratory experiments from Field Z are required to understand the overall dependency of porosity on stresses. The maximum allowable preconsolidated pressure for Field Z is estimated to be 56 MPa (assuming hydrostatic pressure during burial). Based on the sample collected from the nearby

Field X, the preconsolidation pressure is estimated to be about 45 MPa when the volumetric strain experience a drastic change.

For Gulf of Mexico Field X, Chan & Zoback [3] reported a 4.9 percent porosity reduction with respect to the initial porosity after a 55 MPa depletion using the static DARS analysis. If we assume the preconsolidation pressure (or threshold pressure) is indeed 45 MPa, the overstress experienced in Field X will be roughly equal to 10 MPa. From Equation 2, an additional 0.07% volumetric strain per day will be exerted on the formation if the production ceased on the date that the last stress measurement was made.

Unlike Field X, the amount of depletion has yet to reach the threshold pressure, hence a dynamic DARS involving viscoplastic effect is not necessary. Based on the interpretation from the laboratory experiments and the in-situ  $S_{hmin}$  measurements, a DARS analysis for Field Z is conducted (Figure 5). The analysis predicts a 4% change in porosity relative to the initial porosity had occurred when the last stress measurement was made soon after production. Utilizing the porosity-permeability relationship developed in Figure 2, permeability changes from Field Z can be estimated assuming the reservoir will continue to deplete following the same stress path. The blue open circles in Figure 6 are the estimated permeability corresponding to the stress measurements and the initial permeability prior to production. The blue dotted lines are the lower-bound and upper-bound of the permeability prediction based on the two trends derived in Figure 2. In-situ permeability measurements from three different wells in Field Z are available. Well A is located near the center of the reservoir and wells B and C are located near the edge of the reservoir. Permeability measurements in these three wells are collected briefly after production begun (except well B where the first permeability measurement is collected after about 10 MPa of depletion). Without the initial permeability from these wells, we use the average value of the reported permeability from Field Z based on the reservoir quality. Well A has a relatively low permeability and is within the range of permeability for a moderate quality sand interval, while initial permeability for well B and C are estimated to be 470mD (the average value for good reservoir quality sands).

The in-situ permeability for well A seems to follow the lower-bound of the permeability loss while well B and C appear to agree with the upper-bound of permeability loss. Note that the absence of initial permeability for these wells make it quite difficult to know if the prediction is correct. As initial permeability for good quality reservoir sands ranged from 350 to 540 mD, measurements from well B can easily be fitted to the predicted values if the initial permeability used in the analysis is reduced. However, only the average value is used in this case to show that uncertainties associated with in-situ measurements can also affect the accuracy of the DARS prediction.

## 5. CONCLUSIONS

By incorporating the Perzyna viscoplasticity theory to the modified Cam clay cap model, we extended the standard DARS analysis based on static laboratory experiments to a dynamic DARS that includes time-dependent deformations, such as creep, for estimating porosity and permeability changes. Empirical relationships between production-induced compaction and permeability loss were derived based on several laboratory experiments. The two limiting trends derived in this study describe almost 95% of the experimental results. While the physical process controlling the upper bound of the laboratory derived porosity-permeability relationship remains unknown, the lower bound corresponds well to the Kozeny-Carmen relationship for extremely permeable sand. Our case study shows that with adequate information, it is possible to estimate the degree of permeability loss associated with production-induced compaction. A careful and well-planned laboratory study along with in-situ stress measurements are the key to reducing the uncertainties associated with the porosity, permeability and compaction predictions from the DARS analysis. Since most of the porosity and permeability loss associated with depletion are irreversible, stress management may become critical for reservoirs in which inelastic deformations are the dominant mode of reservoir deformation.

## 6. ACKNOWLEDGEMENTS

We thank BP-Amoco for providing the GOM Field Z data used in this study. Financial support for this project was provided by the USGS (Contract No. 2BCZ-418) and the Stanford Rock and Borehole Geophysics project.

## REFERENCES

1. Hagin, P.N. & Zoback, M.D., 2003a. Viscous deformation of unconsolidated reservoir sands (Part I): Time-dependent deformation, frequency dispersion and attenuation, Geophysics, in press.



2. Hagin, P.N. & Zoback, M.D., 2003b. Viscous deformation of unconsolidated reservoir sands (Part II): Linear viscoelastic models, Geophysics, in press
3. Chan, A.W., and Zoback, M.D., 2002, Deformation analysis in reservoir space (DARS): a simple formalism for prediction of reservoir deformation with depletion. SPE 78174.
4. Zhu, W., and Wong, T.F., 1997, The transition from brittle faulting to cataclastic flow: permeability evolution. JGR 102, 3027-3041.
5. Yale, D.P., 2002, Coupled geomechanics-fluid flow modeling: effects of plasticity and permeability alteration. SPE 78202.
6. Crawford, B.R., and Yale, D.P., 2002, Constitutive modeling of deformation and permeability: relationships between critical state and micromechanics. SPE 78189.
7. Hagin, P.N., 2003. Application of Viscoelastic, Viscoplastic, and Rate-and-State Friction Constitutive Laws to the Deformation of Unconsolidated Sands. Unpublished Ph.D. Thesis, Stanford University, 126pp.
8. Hagin, P.N., and Zoback, M.D., 2004. Viscoplastic deformation in unconsolidated reservoir sands (Part 1): Laboratory observations and time-dependent end cap models. ARMA/NARMS 04-567.
9. Desai, C.S. & Siriwardane, H.J. 1984. *Constitutive Laws for Engineering Materials, with Emphasis on Geologic Materials*. Prentice-Hall: Englewood Cliffs, N.J., 468p.
10. Ostermeier, R. M., 2001, Compaction effects on porosity and permeability: deepwater Gulf of Mexico turbidites. JPT. Journal of Petroleum Technology, Feb. 2001, p. 68-74.
11. Carman, P.C., 1961. L'écoulement des Gaz à Travers les Milieux Poreux, Paris: Bibliothèque des Science et Techniques Nucléaires, Press Universitaires de France, 198pp.
12. Mavko, G., Mukerji, T., and Dvorkin, J., 1998, The Rock Physics Handbook: Tools for Seismic Analysis in Porous Media. New York: Cambridge University Press, 329pp.
13. Mavko, G., and Nur, A., 1997. The effect of a percolation threshold in the Kozeny-Carman relation. Geophys., 62, 1480-1482.

...the ... of ...  
...the ... of ...  
...the ... of ...  
...the ... of ...

...the ... of ...  
...the ... of ...

...the ... of ...  
...the ... of ...

...the ... of ...  
...the ... of ...

...the ... of ...  
...the ... of ...

...the ... of ...  
...the ... of ...

...the ... of ...  
...the ... of ...

...the ... of ...  
...the ... of ...

...the ... of ...  
...the ... of ...

...the ... of ...  
...the ... of ...

...the ... of ...  
...the ... of ...

...the ... of ...  
...the ... of ...